https://doi.org/10.52131/jmps.2023.0402.0039

Journal of Materials and Physical Sciences

Volume 4, Number 2, 2023, Pages 92 - 101

Journal Homepage:
https://journals.internationalrasd.org/index.php/jmps

JOURNAL OF MATERIALS AND PHYSICAL SCIENCES
INTERNATIONAL RESEARCH ASSOCIATION FOR SUSTAINABLE DEVELOPMENT

First Principles Study of Structral, Electronic, and Optical Proeprties of Lead Free Double Perovskites Rb2LiTlX6 (X = Cl, Br, I) for Optoelectronics Applications

Ahmad Ayyaz[1], Ahmad Usman[1], Q. Mahmood[2,3*], Ayesha Ihsan[4], Faseeh ur Raheem[5]

[1] Centre for Advanced Studies in Physics, GC University, Lahore, Pakistan
[2] Basic and Applied Scientific Research Center, Imam Abdulrahman Bin Faisal University, P.O. Box 1982, Dammam, 31441 Saudi Arabia
[3] Department of Physics, College of Science, Imam Abdulrahman Bin Faisal University, P.O. Box 1982, Dammam, 31441 Saudi Arabia
[4] Department of Physics, Government College University, Faisalabad 38000, Pakistan
[5] Institute of Physics, The Islamia University of Bahawalpur, Pakistan

ARTICLE INFO

Article History:
Received: October 04, 2023
Revised: November 28, 2023
Accepted: December 29, 2023
Available Online: December 31, 2023

Keywords:
Band gap
Density Fuctional Theory
Solar cells
Optoelectronics

ABSTRACT

The presently, the renewable energy becomes the important source in the world because of shortage of oil and fossil sources and their hazardous. The solar cell is the main frontiers of cheap and clean renewable energy. We have chosen to lead free double perovskites Rb_2LiTlX_6 (X = Cl, Br, I) for structural, electronic, and optical applications because of their stable structure and direct band gaps. For the calculations, the modified Becke and Johnson potential has been applied (mBJ). The lattice constants are increase from Cl to I while bulk modulus decreases. The phase stability ensures the cubic phase with space group 221_Fm3m. The band structures and density of states show the band gabs (2.62, 1.39, & 0.14) eV. The ideal band gap of $Rb_2LiTlBr_6$ ensure the absorption of light in the visible region which has significant importance for solar cells applications.

*Corresponding Author's Email: qmmustafa@iau.edu.sa

1. Introduction

To meet the challenge of energy crisis, variety of sources has been assessed and found the conversion of sun light into direct electrical energy is the clean source, cheap, environment friendly and long-term source of energy (Biswas et al., 2012). The researchers are putting their best efforts to explore the materials which are highly efficient, easily available, and non-toxic. During last decade, tremendous work has been done to optimize the materials for solar cells and found the Lead based perovskites halides has achieved record energy conversion efficiency 23% (Shah et al., 2020; Siddique et al., 2019). Later, the single layered junction solar cells in 2009 are investigated with efficiency of 28% ($H_2NCHNH_2PbX_3$) and double junction solar cells of tin halide ($CH_3NH_3SnI_3$) with efficiency 31.1% (Pei et al., 2011). The improving struggle explored the organic and inorganic based double perovskites with optimal efficiency 35% (Hong, Yuan, & Liu, 2020). Now we want to explore the stable double perovskites with maximum efficiency and low-cost materials.

Even though the high-power conversion efficiency materials are scrutinized but their existing challenges limit their applicability for commercial applications. The problems of these materials which are needed to address; instability and presence of lead which is very toxic for environment (Peng et al., 2011). Therefore, during last few years, huge efforts are done on lead-free perovskites and double perovskites as a potential replacement of $MAPbI_3$ (MA = CH_3NH_3), Cs_2PbX_6 (X = Cl, Br, I) and vacancy-ordered double perovskites (Heremans et al., 2008; Poudel et al., 2008; Tritt, 2011). From all the family of lead-free double

perovskites, the perovskites based on Bi/Ag are considered more stable and environmentally friendly as a substituent of $MAPbI_3$. Even though the Bi and Ag DPs have band gap in the visible region of spectrum (1.9 eV to 2.3 eV) but indirect gap which is not favorable for solar cell applications (Kaur & Kumar, 2016). The indirect band gap semiconductors reduce the oscillator strength for radiative recombination and absorption of light that demands thicker absorber layer like silicon. This thicker layer is very tricky for low mobility charge carriers. Therefore, we must need develop new class of Pb free DPs which have direct nature of band gap.

To above mentioned problems of highly efficient solar cell materials, the theoretical and experimental research testify the list of double perovskites. The study of $Cs_2AgBiBr_6$ open the new doors of double perovskites like $Cs_2InSbCl_6$, $Rb_2AgInBr_6$, $Rb_2CuInCl_6$ etc. that have band gaps comparable to $MAPbI_3$ complement (Reshak, 2016). Young et al, studied the lead-free nanocrystals of $Cs_2AgIn_xBi_{1-x}Cl_6$ with doping concentration of In as X = 0, 0.25, 0.5, 0.75 and 0.9. The indirect bad gap has been tuned to direct band gap of value at X = 0.75. The direct band gap has three time more absorption cross-section and five times more efficiency as associated to indirect band gap semiconductors. In these double perovskites, we have found 36.6% photoluminescence quantum efficiency for direct band gap nanocrystals (Kanatzidis, 2010).

The analysis of various physical properties of the materials such as perovskites and double perovskite crystal structure, band structure and stability has got considerable attention in the scientific community working in the field of material sciences. In the direction for having better understanding of different aspects of the materials many approximation methods are applied, which subjected to the highly efficient computer programming such as the VASP/Quantum Espresso software are widely used for that purpose. These software's are highly capable to construct the graphical representation of band structural, electronic, and thermoelectric structures for the practical purposes. We can study these properties by taking number constraints into account such as pressure, temperatures and creating vacancies. It has been found that newly crystalline phases are induced in the presence of external pressure and temperature. These theoretical techniques will be applied here to analyze electric and thermoelectric aspects of the perovskite and DPs materials. With the above-mentioned software's, we will construct the graphical interpretations of the different physical properties of the perovskite and double perovskite materials for solar cell applications.

2. Method of Calcualtions

Using first principle calculations based on density functional theory (DFT), our main focus is to study and design perovskite and double perovskite materials with excellent electronic properties, high thermal/electrical conductivity, power factor and figure of merit at different temperature essential for efficient optoelectronic and thermoelectric device applications. DFT is the most successful and accurate techniques used to investigate the ground state properties of materials such as semiconductors, insulators, and metals. It was developed in 1964 and described by two theorems (presented by Hohenberg and Kohn) (Hong et al., 2016).

To explore the electronic properties of perovskite and double perovskite materials, we will use different DFT based packages such as VASP (Snyder & Toberer, 2008), Quantum ESPRESSO (Liu et al., 2012) and Wien2k (Wolf, Hinterding, & Feldhoff, 2019). As DFT has some limitations, show failure for excited states properties and underestimates the band gap considerably, predicts a material as a semimetal instead of its experimentally found insulating nature. As a result, more sophisticated hybrid functional particularly PBE0 and HSE06 (Snyder & Toberer, 2008) employed for calculating accurate band gap, will be used to overcome these shortcomings. Additionally, phonon calculations will be performed to confirm the stability of the systems. For these systems, the thermoelectric response at different temperatures will be calculated using BoltzTraP package (Khandy & Gupta, 2020), which has been interfaced with VASP, Wien2k and Quantum ESPRESSO packages. The figure of merit may be presented as:

$$zT = \frac{S^2 \sigma \tau}{\kappa} \quad (1)$$

In equation (2) S is the Seebeck coefficient followed as [22]

$$S = \frac{\kappa_\beta}{e\sigma(T)} \int_{-\infty}^{+\infty} dE\sigma(E) \frac{E-\mu df(E-\mu)}{TdE} \quad (2)$$

where σ electrical conductivity.

$$\sigma(T) = -\int_{-\infty}^{+\infty} dE\sigma(E) \frac{df(E-\mu)}{TdE} \quad (3)$$

Where f, $\tau(E)$, μ, V(E) and κ represent the Fermi function, the scattering time, V (E) is the Fermi velocity, the chemical potential and thermal conductivity respectively. It consists of both lattice (κ_l) and electronic thermal conductivity (κ_{el}). Vibrational properties for these materials will also be investigated for revising various remarkable physical properties.

3. Results and Discussion

3.1. Structral Properties

Figure 1 displays the atomic bonding view and octahedral aspect of the cubic crystal arrangement (Fm3¯m_No.225). This framework consists of a pair of cations (Li, Tl) and one of three anions (Cl, Br, I), which combine to create octahedrons. The octahedrons of sodium and thallium are divided into 12 coordinated places. The spaces of octahedrons are filled by Rb atoms (Cai, Hu, Zhuang, & Li, 2019). The structures are optimized for volume and lattice properties using energy convergence. The calculated lattice constant (a_o) demonstrates a rising pattern from chlorine to iodine due to the larger size of the halide ions. The Bulk modulus drops as halide ions descend the periodic group, resulting in decreased material hardness (Refer to Table 1).

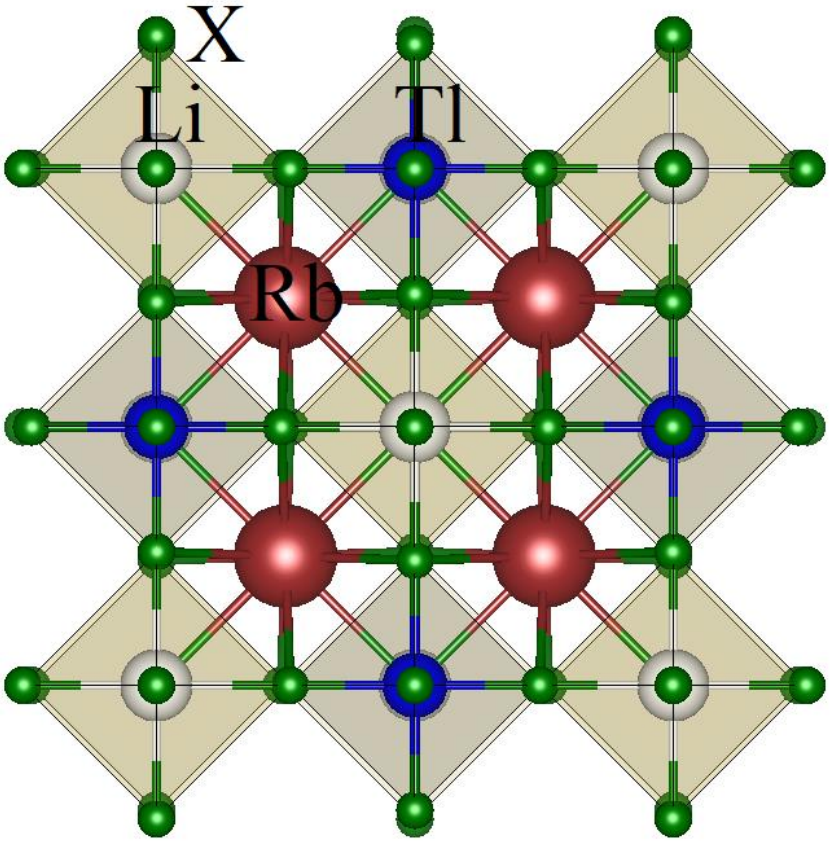

Figure 1: Cubic Structural configuration of Rb_2LiTlX_6 (X = Cl, Br, I)

The stability of the structures has been calculated by Goldschmidt relation $t = (r_{Rb} + r_X)/\sqrt{2}(r_{Li/Tl} + r_X)$, Here r_{Rb}, $r_{Li/Tl}$ and r_X, are the radii of Cs, Li, Tl, and X atoms (Ayyaz, Murtaza, Naeem, et al., 2024). The accurate value of tolerance factor is from 0.90 to 1.04 and any less or more values form this limit introduce the instability. The values in Table 1 report the studied materials are highly stable. Moreover, the formation energy has been calculated from the following relation $H_f = E_{(Rb_aLi_bTl_cX_d)} - (aE_{Rb} + bE_{Li} + cE_{Tl} + dE_X)$, where $E_{(Rb_aLi_bTl_cX_d)}$, E_{Rb}, E_{Li}, E_{Tl}, and E_X are the energies of Rb, Li, Tl, and X atoms (Fedorovskiy, Drigo, & Nazeeruddin, 2020). The calculated heat of formation is shown in Table 1, with the negative value indicating the release of energy during compound synthesis (Huma et al., 2021; Ju et al., 2018; Mahmood, Ghrib, Rached, Laref, & Kamran, 2020). The values drop from Cl to I, indicating that chlorides are more suitable for compound production than bromides and iodides.

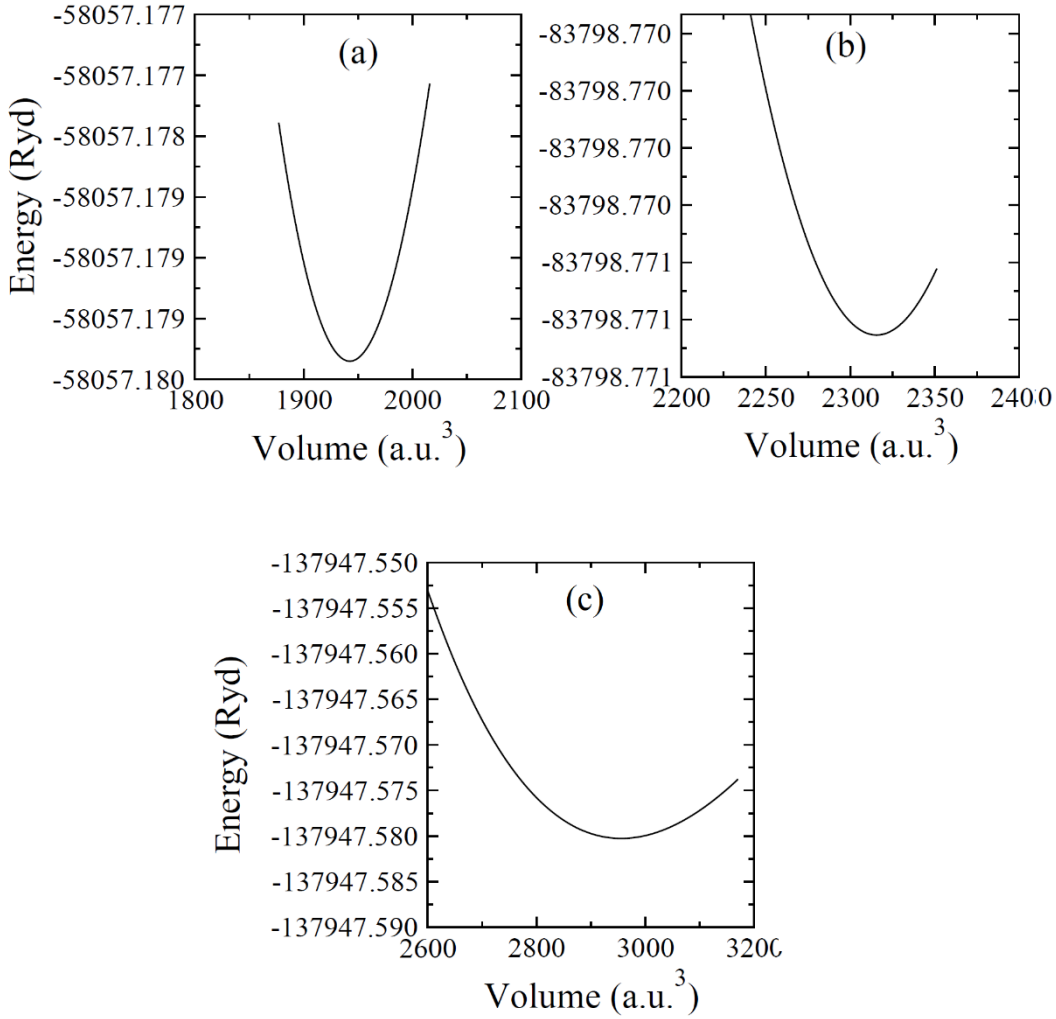

Figure 2: Optimization plots for Rb_2LiTlX_6 (X = Cl, Br, I) showing ground state volume and energy

Table
The calculated parameters for Rb_2LiTlX_6 (X = Cl, Br, I)

Parameters	$Rb_2LiTlCl_6$	$Rb_2LiTlBr_6$	Rb_2LiTlI_6
a_o (Å)	10.48	11.11	12.06
B (GPa)	25.23	19.25	14.24
ΔH_f (eV)	-2.4	-2.0	1.35
t_F	0.98	0.95	0.92
***E_g* (eV)**	2.62	1.39	0.21
$\varepsilon_1(0)$	2.77	3.42	5.47
***n* (0)**	1.66	1.85	2.33
R (0)	0.062	0.089	0.166

3.2. Electronic properties

The band structures of the given compounds has been formulated in the Fig.3 (a-c). The BG at Γ have been identified as 2.62, 1.39 and 0.21 eV for $Rb_2LiTlCl_6$, $Rb_2LiTlBr_6$, and Rb_2LiTlI_6, respectively (refer to Table 1). The significant decrease in band gap caused by the different halide ions ranging from Cl to I makes them suitable for many optoelectronic and energy-related applications (Ullah, Ali, Murtaza, Khan, & Mahmood, 2020; Ullah, Ali, Murtaza, Mahmood, & Ramay, 2020). States in the valence band are dense and closely packed within the energy range of zero to -1.0 eV, but the conduction band edge contains only one state, which is suppressed by the growing ionic size of halide ions.

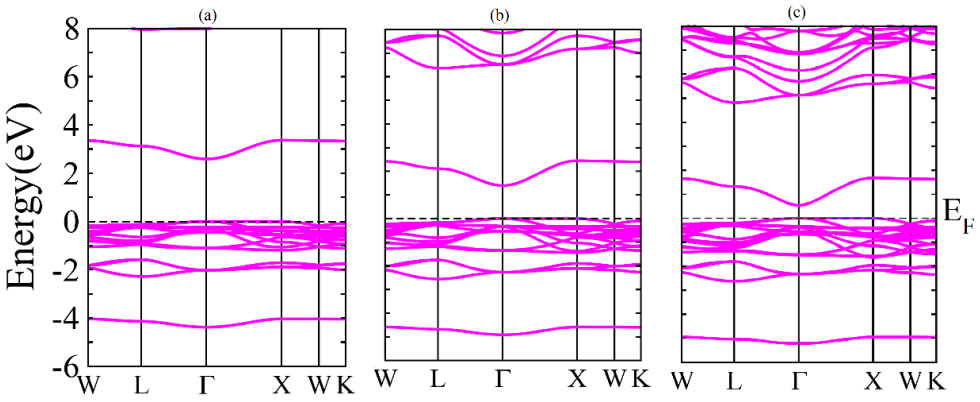

Figure 3: Band gap arrangement of Rb_2LiTlX_6 (X = Cl, Br, I)

The flat valence band states and curved conduction band states result in holes having much larger effective masses in the valence band in comparison to electrons in the conduction band. This also depicts the p-type semiconducting nature of these materials. Furthermore, the transitions and recombination of carriers across the band gap have been explained by DOS, whose total values for compounds are plotted in Fig. 4 (a-c). and separate valence states of Rb, Li, Tl and halogen ions are plotted in Fig. 5 (a-c). The halogen atoms (Cl/Br/I) have significant contribution in the electronic transition and in optical performance of the studied materals.

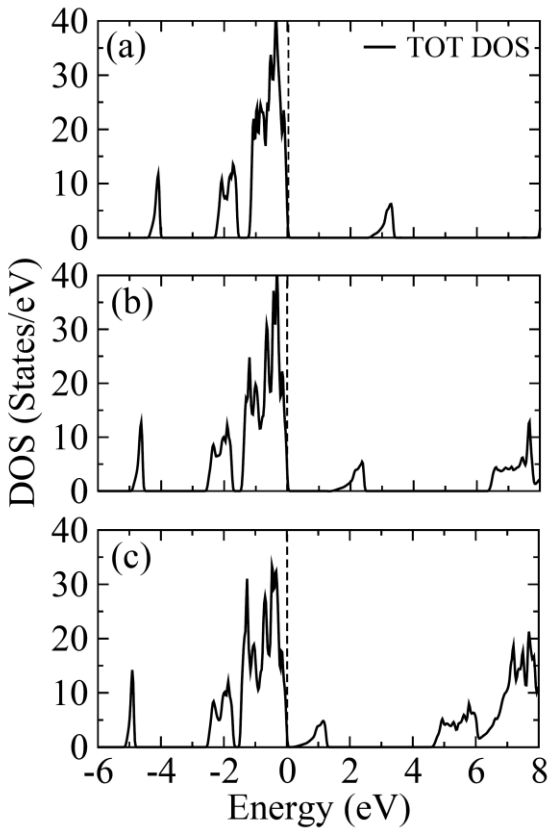

Figure 4: TDOS of (a) $Rb_2LiTlCl_6$ (b) $Rb_2LiTlBr_6$ and (c) Rb_2LiTlI_6

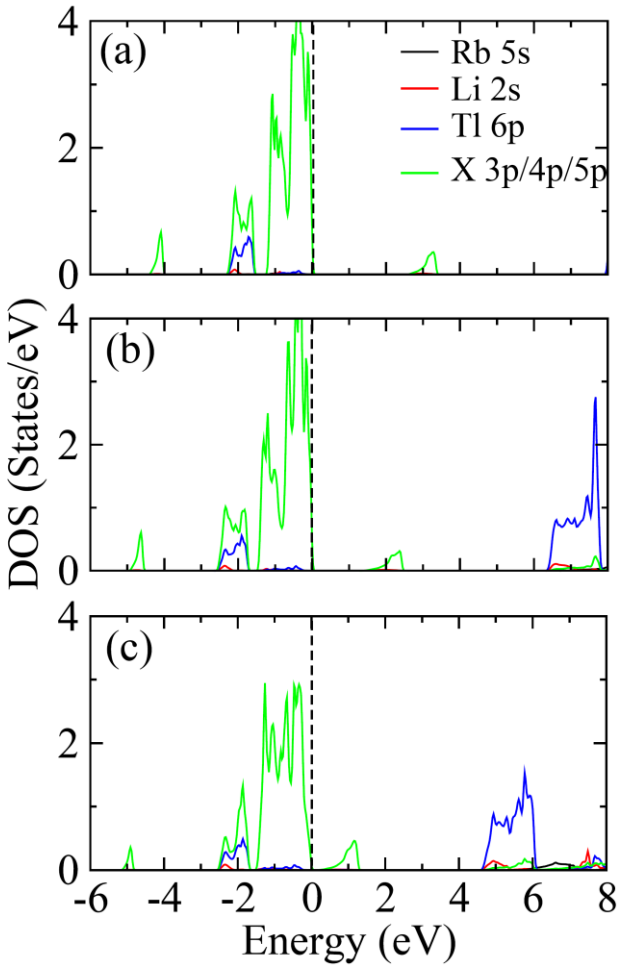

Figure 5: PDOS of (a) $Rb_2LiTlCl_6$ (b) $Rb_2LiTlBr_6$ and (c) Rb_2LiTlI_6

3.3. Optical Properties

The photovoltaic characteristics of materials are determined by the band gap, energy absorption, and efficiency in processing light into electricity. Fig. 7 displays the optical properties of the studied substances within the energy range of 0–6 eV. The optical properties of Rb_2LiTlX_6 (X = Cl, Br, I) compounds have been characterized by the real and imaginary dielectric coefficients, $\varepsilon_1(\omega)$ and $\varepsilon_2(\omega)$, respectively (Blaha, Schwarz, Madsen, Kvasnicka, & Luitz, 2001; Zhang et al., 2003), which vary with energy. This also encompasses the energy which materials either attenuate or absorbed (Alreyahi et al.; Jiang et al., 2016).

Fig. 6 (a) presents the calculated real portion of the dielectric constant for $Rb_2LiTlCl_6$, $Rb_2LiTlBr_6$, and Rb_2LiTlI_6. This component characterizes how the material scatters entering photons. The static value of $\varepsilon_1(\omega)$ for $Rb_2LiTlCl_6$, $Rb_2LiTlBr_6$, and Rb_2LiTlI_6 are 2.9, 3.5, and 5.5, respectively, which increases as the band gap decreases (Ayyaz, Murtaza, Ahmed, et al., 2024). Moreover, the examined perovskites exhibit maximum $\varepsilon_1(\omega)$ values within the visible area. The refractive index $n(\omega)$ indicates how light travels across the investigated materials (Ayyaz, Murtaza, Shafiq, et al., 2023). The refractive indices at zero frequency, $n(0)$, for $Rb_2LiTlCl_6$, $Rb_2LiTlBr_6$, and Rb_2LiTlI_6 are 1.4, 1.70, and 1.82. Fig. 6 (b) displays peak $n(\omega)$ values in 1.7-2.4 eV in the observed photon energy range. The correlation between $\varepsilon_1(\omega)$ and $n(\omega)$ reveals similar graph trends with greater energy, confirming the reliability of the results (Ayyaz, Murtaza, Usman, et al., 2024).

Fig. 6 (c) shows the trend of $R(\omega)$ and the computed static reflectance measurements $R(0)$ for $Rb_2LiTlCl_6$, $Rb_2LiTlBr_6$, and Rb_2LiTlI_6 found below 20%. The values of $R(\lambda)$ in the visible range are also below 20%. All the examined double perovskites, $Rb_2LiTlCl_6$, $Rb_2LiTlBr_6$, and Rb_2LiTlI_6, have shown the highest capacity of absorbing visible light. Fig. 6(d) displays a graph showing the optical energy loss $L(\omega)$ for $Rb_2LiTlCl_6$, $Rb_2LiTlBr_6$, and Rb_2LiTlI_6 double perovskites, indicating very low values (below 35%). These

materials absorb most of the incoming energy (Kibbou, Haman, Essaoudi, & Ainane, 2023). After a thorough examination of several perovskite materials, such as $Rb_2LiTlCl_6$, $Rb_2LiTlBr_6$, and Rb_2LiTlI_6, it is being shown that they are crucial for solar cells due to their optical properties.

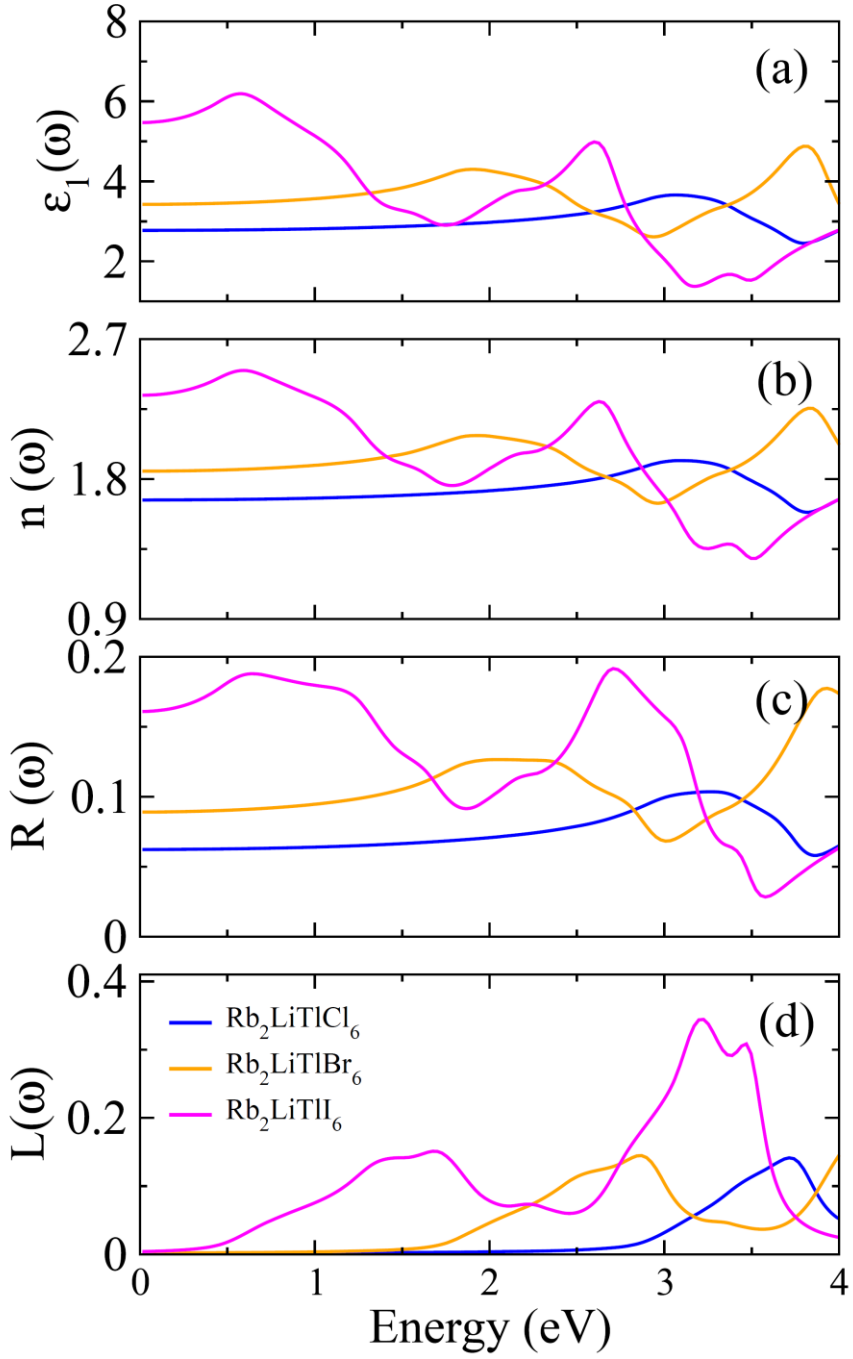

Figure 6: The optical parameters $\varepsilon_1(\omega)$, $n(\omega)$ $R(\omega)$, & $L(\omega)$ for Rb_2LiTlX_6 (X = Cl, Br, I)

Fig.7 (a) illustrates the link between the value of $\varepsilon_2(\omega)$ and energy. The symbol $\varepsilon_2(\omega)$ denotes the optical band gap and absorption characteristics. There is no absorption evidence seen up to energies below band gap for the above compounds, indicating that the expected electronic and optical bandgaps are quite similar. Moreover, $\alpha(\omega)$, $k(\omega)$, and $\sigma(\omega)$ shows the identical pattern to $\varepsilon_2(\omega)$, as shown in Figure 7 (b-d). Two parameters $\alpha(\omega)$ and $k(\omega)$ goven the absorbing capability of the material whereas $\sigma(\omega)$ indicates the movement of charge carriers (Ayyaz, Murtaza, Umer, Usman, & Raza, 2023). Due to similar pattern, $\alpha(\omega)$, $k(\omega)$, and $\sigma(\omega)$ have the greatest values at energy levels of. Therefore, these findings suggest that these materials can be utilized in optoelectronic devices and aslo for solar energy harvesting applications.

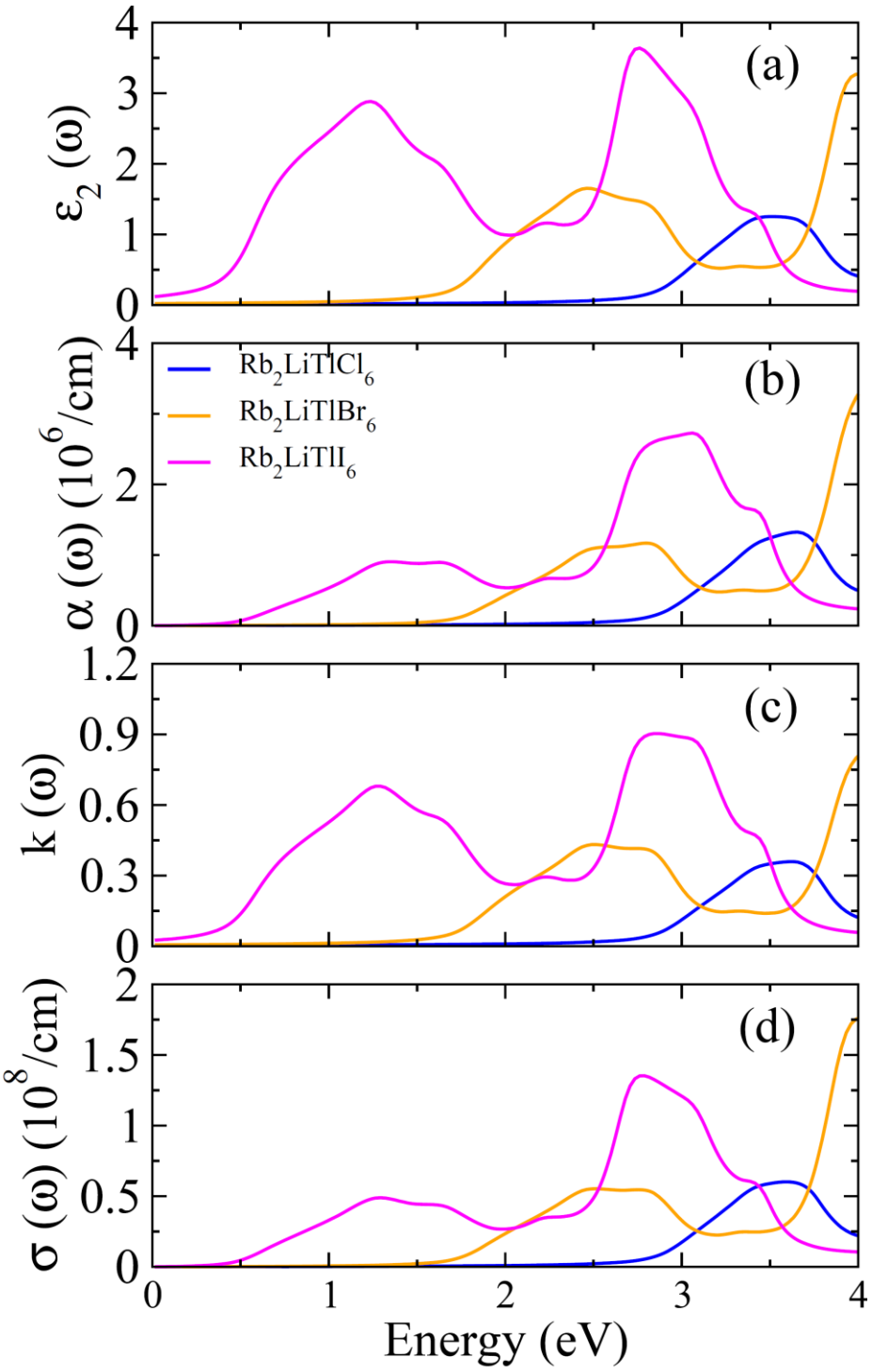

Figure 7: The optical parameters ε₂(ω), α(ω), k(ω), and σ(ω) for Rb_2LiTlX_6 (X = Cl, Br, I)

4. Conclusion

In short, electronic, optical, and thermoelectric properties of Rb_2TiCl_6 and Rb_2TiBr_6 double perovskites are addressed by first principle calculations. The structural and thermodynamic stabilities of both compounds confirmed tolerance factor (0.89-0.96), and, negative enthalpy of formation, respectively. The band structures and density of states show indirect band gaps 2.62 eV, 1.39 eV, and 0.21 eV for Rb_2TiCl_6, Rb_2TiBr_6 and Rb_2TiI_6, respectively. The detailed optical properties show the absorption of light energy is shifted from ultraviolet region to infrared region. The band gap Rb_2TiBr_6 of is considered ideal for solar cell applications. Moreover, minimum values of optical and reflectivity also increase their significance for optoelectronic and solar cell applications.

Reference

Alreyahi, A. Y., Al Azar, S., Mousa, A. A., Essaoud, S. S., Berarma, K., Maghrabi, M., . . . Mufleh, A. The Electronic, Optical, Thermoelectric, and Structural Properties of a Cubic Double Perovskite X2agbibr6 (X= Li, Na, K, Rb, Cs): Ab-Initio Calculation. *Optical, Thermoelectric, and Structural Properties of a Cubic Double Perovskite X2agbibr6 (X= Li, Na, K, Rb, Cs): Ab-Initio Calculation*.

Ayyaz, A., Murtaza, G., Ahmed, A., Ramay, S. M., Usman, A., Farid, G., & Naeem, M. (2024). Comparative DFT-based investigation of physical properties of Cs2MBiBr6 (M= Ag, Cu, and Au) Perovskites: Sustainable materials for renewable energy. *Computational Condensed Matter, 38*, e00885.

Ayyaz, A., Murtaza, G., Naeem, M., Usman, A., Ramay, S. M., Irfan, M., & Irfan, H. (2024). DFT exploration of elastic, optoelectronic, and thermoelectric properties of stable and eco-friendly double perovskites Cs2YAuX6 (X= Cl, Br) for green energy applications. *Journal of Physics and Chemistry of Solids*, 111936.

Ayyaz, A., Murtaza, G., Shafiq, M., Shah, M. Q., Sfina, N., & Ali, S. (2023). Exploring structural, thermodynamic, elastic, electro-optic, and thermoelectric characteristics of double perovskites Rb2XInBr6 (X= Na, K) for photovoltaic applications: A DFT approach. *Solar Energy, 265*, 112131.

Ayyaz, A., Murtaza, G., Umer, M., Usman, A., & Raza, H. H. (2023). Structural, elastic, optoelectronic, and transport properties of Na-based halide double perovskites Na2CuMX6 (M= Sb, Bi, and X= Cl, Br) as renewable energy materials: a DFT insight. *Journal of Materials Research, 38*(20), 4609-4624.

Ayyaz, A., Murtaza, G., Usman, A., Umer, M., Shah, M. Q., & Ali, H. S. (2024). First principles insight on mechanical stability, optical and thermoelectric response of novel lead-free Rb2ScCuBr6 and Cs2ScCuBr6 double perovskites. *Materials Science in Semiconductor Processing, 169*, 107910.

Biswas, K., He, J., Blum, I. D., Wu, C.-I., Hogan, T. P., Seidman, D. N., . . . Kanatzidis, M. G. (2012). High-performance bulk thermoelectrics with all-scale hierarchical architectures. *Nature, 489*(7416), 414-418.

Blaha, P., Schwarz, K., Madsen, G. K., Kvasnicka, D., & Luitz, J. (2001). wien2k. *An augmented plane wave+ local orbitals program for calculating crystal properties, 60*(1).

Cai, B., Hu, H., Zhuang, H.-L., & Li, J.-F. (2019). Promising materials for thermoelectric applications. *Journal of Alloys and Compounds, 806*, 471-486.

Fedorovskiy, A. E., Drigo, N. A., & Nazeeruddin, M. K. (2020). The role of Goldschmidt's tolerance factor in the formation of A2BX6 double halide perovskites and its optimal range. *Small Methods, 4*(5), 1900426.

Heremans, J. P., Jovovic, V., Toberer, E. S., Saramat, A., Kurosaki, K., Charoenphakdee, A., . . . Snyder, G. J. (2008). Enhancement of thermoelectric efficiency in PbTe by distortion of the electronic density of states. *Science, 321*(5888), 554-557.

Hong, A., Li, L., He, R., Gong, J., Yan, Z., Wang, K., . . . Ren, Z. (2016). Full-scale computation for all the thermoelectric property parameters of half-Heusler compounds. *Scientific reports, 6*(1), 22778.

Hong, A., Yuan, C., & Liu, J. (2020). Quaternary compounds Ag2XYSe4 (X= Ba, Sr; Y= Sn, Ge) as novel potential thermoelectric materials. *Journal of Physics D: Applied Physics, 53*(11), 115302.

Huma, M., Rashid, M., Mahmood, Q., Algrafy, E., Kattan, N. A., Laref, A., & Bhatti, A. (2021). Physical properties of lead-free double perovskites A2SnI6 (A= Cs, Rb) using ab-initio calculations for solar cell applications. *Materials Science in Semiconductor Processing, 121*, 105313.

Jiang, S., Fang, Y., Li, R., Xiao, H., Crowley, J., Wang, C., . . . Baikie, T. (2016). Pressure-dependent polymorphism and band-gap tuning of methylammonium lead iodide perovskite. *Angewandte Chemie International Edition, 55*(22), 6540-6544.

Ju, D., Zheng, X., Yin, J., Qiu, Z., Türedi, B., Liu, X., . . . Bakr, O. M. (2018). Tellurium-based double perovskites A2TeX6 with tunable band gap and long carrier diffusion length for optoelectronic applications. *ACS Energy Letters, 4*(1), 228-234.

Kanatzidis, M. G. (2010). Nanostructured thermoelectrics: The new paradigm? *Chemistry of materials, 22*(3), 648-659.

Kaur, K., & Kumar, R. (2016). Effect of pressure on electronic and thermoelectric properties of magnesium silicide: A density functional theory study. *Chinese Physics B, 25*(5), 056401.

Khandy, S. A., & Gupta, D. C. (2020). Magneto-electronic, mechanical, thermoelectric and thermodynamic properties of ductile perovskite Ba2SmNbO6. *Materials Chemistry and Physics, 239*, 121983.

Kibbou, M., Haman, Z., Essaoudi, I., & Ainane, A. (2023). Designing new halide double perovskite materials Rb2AgGaX6 (X: Br, Cl) with direct band gaps and high power conversion efficiency. *Journal of Solid State Chemistry, 317*, 123698.

Liu, H., Shi, X., Xu, F., Zhang, L., Zhang, W., Chen, L., . . . Snyder, G. J. (2012). Copper ion liquid-like thermoelectrics. *Nature materials, 11*(5), 422-425.

Mahmood, Q., Ghrib, T., Rached, A., Laref, A., & Kamran, M. (2020). Probing of mechanical, optical and thermoelectric characteristics of double perovskites Cs2GeCl/Br6 by DFT method. *Materials Science in Semiconductor Processing, 112*, 105009.

Pei, Y., Shi, X., LaLonde, A., Wang, H., Chen, L., & Snyder, G. J. (2011). Convergence of electronic bands for high performance bulk thermoelectrics. *Nature, 473*(7345), 66-69.

Peng, H., Wang, C.-L., Li, J.-C., Zhang, R.-Z., Wang, H.-C., & Sun, Y. (2011). Theoretical investigation of the thermoelectric transport properties of BaSi2. *Chinese Physics B, 20*(4), 046103.

Poudel, B., Hao, Q., Ma, Y., Lan, Y., Minnich, A., Yu, B., . . . Vashaee, D. (2008). High-thermoelectric performance of nanostructured bismuth antimony telluride bulk alloys. *Science, 320*(5876), 634-638.

Reshak, A. (2016). Thermoelectric properties of highly-mismatched alloys of GaN x As 1− x from first-to second-principles methods: energy conversion. *RSC advances, 6*(76), 72286-72294.

Shah, S. H., Murtaza, G., Baz, A., Algrafy, E., Laref, A., & Kattan, N. A. (2020). Study of anion replacement effect on SrCd2X2 (X= P, As, Sb, Bi) compounds by FPLAPW+ lo. *Materials Science in Semiconductor Processing, 119*, 105290.

Siddique, M., Rahman, A. U., Iqbal, A., Haq, B. U., Azam, S., Nadeem, A., & Qayyum, A. (2019). A systematic first-principles investigation of structural, electronic, magnetic, and thermoelectric properties of thorium monopnictides Th Pn (Pn= N, P, As): a comparative analysis of theoretical predictions of LDA, PBEsol, PBE-GGA, WC-GGA, and LDA+ U Methods. *International Journal of Thermophysics, 40*, 1-21.

Snyder, G. J., & Toberer, E. S. (2008). Complex thermoelectric materials. *Nature materials, 7*(2), 105-114.

Tritt, T. M. (2011). Thermoelectric phenomena, materials, and applications. *Annual review of materials research, 41*, 433-448.

Ullah, R., Ali, M. A., Murtaza, G., Khan, A., & Mahmood, A. (2020). Ab initio study for the structural, electronic, magnetic, optical, and thermoelectric properties of K2OsX6 (X= Cl, Br) compounds. *International Journal of Energy Research, 44*(11), 9035-9049.

Ullah, R., Ali, M. A., Murtaza, G., Mahmood, A., & Ramay, S. M. (2020). The significance of anti-fluorite Cs2NbI6 via its structural, electronic, magnetic, optical and thermoelectric properties. *International Journal of Energy Research, 44*(13), 10179-10191.

Wolf, M., Hinterding, R., & Feldhoff, A. (2019). High power factor vs. high zT—A review of thermoelectric materials for high-temperature application. *Entropy, 21*(11), 1058.

Zhang, M., Dai, X., Hu, H., Liu, G., Cui, Y., Liu, Z., . . . Wu, G. (2003). Search for new half-metallic ferromagnets in semi-Heusler alloys NiCrM (M= P, As, Sb, S, Se and Te). *Journal of Physics: Condensed Matter, 15*(46), 7891.